Pharmaceutical Research, Vol. 23, No. 9, September 2006 (© 2006)
DOI: 10.1007/s11095-006-9049-7

Research Paper

Population Pharmacokinetic/Pharmacodynamic Modelling of the Analgesic Effects of Tramadol in Pediatrics

María J. Garrido,[1] Walid Habre,[2] Ferdinand Rombout,[3] and Iñaki F. Trocóniz[1,4]

Received November 25, 2005; accepted May 3, 2006; published online August 9, 2006

Background and Purpose. The efficacy of tramadol (T) in children is not clearly understood because it is still unknown the ability of that population to form the active metabolite O-demethyltramadol (M1) and, whether or not the parent compound has a contribution to the efficacy. The aim was to develop a population pharmacokinetic/pharmacodynamic model for T in pediatrics, identifying the main active components.
Materials and Methods. One hundred four children, mean age (4.55 years) received intravenously 1 mg/kg dose of T over 2.5 min at the end of surgery. If pain relief was inadequate, then an additional 0.33 mg/kg dose was given at 15, 30 and/or 45 min. Plasma samples and analgesic responses such as crying and movement were measured during a 6-h period.
Results. The estimates of the apparent volumes of distribution of the central compartment and at steady state and total plasma clearance of T were 8 l, 46.2 l, and 15.2 l/h, respectively. M1 formation clearance represented only a minor elimination pathway of T. Effect site concentrations of T and M1 were found to be the best predictors of the movement and crying responses, respectively. Steady-state plasma concentration levels of T and M1 of 100 and 15 ng/ml were associated with a 95% probability of adequate pain relief.
Conclusions. Children have the ability to produce enough M1 to achieve proper pain relief. The response variables investigated give further evidence that not only the opioid effects of the metabolite are relevant, also the non-opiod effects of tramadol seem to give a significant contribution in its clinical use.

KEY WORDS: children; NONMEM; population pharmacokinetic/pharmacodynamic modelling; tramadol.

INTRODUCTION

Tramadol (T) is a centrally acting analgesic used widely in the treatment of chronic and acute pain with an efficacy and potency comparable to codeine and pethidine (1,2). T is administered as a racemic mixture of (+)−, and (−)−T which are extensively metabolised in the liver giving among others, the (+)−, and (−)−O-demethyltramadol (M1) active metabolites via CYP2D6 elimination (3,4). The pharmacodynamic (pd) properties of T enantiomers and their M1 metabolites are very different (5–7). The values of the inhibitory μ-opioid binding constants for (+)−T, (−)−T, (+)−M1, and (−)−M1 are 4.1×10^{-6}, 2×10^{-4}, 2.2×10^{-8}, and 1.9×10^{-6} mol/l, respectively. With regard to the inhibition of the noradrenaline (NA) and serotonin (5-HT) re-uptake the corresponding values are 6.9×10^{-6}, 5.9×10^{-7}, 4.2×10^{-5}, and 1.8×10^{-6} mol/l, and 8.7×10^{-7}, 4.8×10^{-6}, 7.5×10^{-6}, and 4.3×10^{-5} mol/l, respectively (7). Since the inhibition of 5-HT and NA re-uptake enhances the inhibitory effects elicited by μ-opioid agonists on pain transmission in the spinal cord (8), description and prediction of the time course of the analgesic response after T administration represents a challenge.

Recently a population pharmacokinetic (pk) model of T and M1 in neonates and young children has been published (9). However, a model relating dose with response through a pharmacokinetic/pharmacodynamic (pk/pd) model has not been yet established.

The purpose of the current study is therefore to develop a population pk/pd model for T in the pediatric population with the aim of identifying the main active components and their functional relationship with the analgesic response, as well as the individual characteristics with a clinical significant effect on such a relationship. Several recent papers have shown that, at least experimentally, the pk/pd approach is suitable to identify the main components in the response elicited after T administration (10–12).

[1] Department of Pharmacy and Pharmaceutical Technology, School of Pharmacy, University of Navarra, Apartado 177, Pamplona, Spain.
[2] Pediatric Anesthesia Unit, Geneva Children's Hospital, Geneva, Switzerland.
[3] Department of Modelling and Simulation, Grünenthal GmbH, Aachen, Germany.
[4] To whom correspondence should be addressed. (e-mail: itroconiz@unav.es)

MATERIALS AND METHODS

Study Design

The data analyzed in the current report came from one hundred and four Caucasian children participating in a randomized, double-blind, multi-center clinical study designed to evaluate the analgesic efficacy and safety of intravenous T in the treatment of postoperative pain in children. Nineteen European centers were involved, and the study protocol was approved by the Local Health Authority and Ethics Committee. During the day of admission, the protocol was explained to the parent or legal guardian and their informed consent was obtained in writing.

Children aged 2 to 8 years, admitted for elective abdominal or urological surgery and requiring the use of intravenous opioids for postoperative analgesia were eligible to participate in the present study. Children were allowed to receive midazolam for pre-medication. Induction of general anesthesia was either via inhalation (sevoflurane or halothane) or intravenously (propofol). Anesthesia was maintained by isoflurane or sevoflurane with controlled ventilation using nitrous oxide/oxygen in all study patients. Intraoperative analgesia was achieved with fentanyl with the last dose to be given at the latest 30 min prior to the administration of the investigational product. Any other analgesic, hypnotic or sedative pre- or co-medications were considered as exclusion criteria. Table I lists the patient characteristics of the population studied. Aminoglycosides, cephalosporins, penicillins, and sulphonamides were the type of anti-microbials drugs given after surgery. With regard the gatrointestinal agents, ondansetron, tropisetron, ranitidine, and metoclopramide were the drugs administered.

Table I. Summary of Individual and Study Characteristics

Characteristic	Value
Demographics	
Age (year)	4.71 (2–8)
Height (cm)	110.0 (80–144)*
Weight (kg)	19.8 (10–43)
Sex	
Female	$n = 28$
Male	$n = 76$
Surgery	
Type	
Urogenital	$n = 96$
Gastrointestinal	$n = 8$
Duration (minutes)	87.3 (28–380)
Opioids	
Fentanyl	$n = 70$
Alfentanyl	$n = 16$
Co-medications given after surgery	
NSAIDs**	$n = 45$
Opioids**	$n = 29$
Diuretics	$n = 7$
Anti-microbials	$n = 53$
Gastrointestinal drugs	$n = 24$

Values are median and ranges in parenthesis unless n is indicated. *, Computed from 99 patients; **, Drugs given ≥ 60 min after the start of the first T infusion.

Drug Administration

At the time of skin closure, a 1 mg/kg dose of T was given intravenously in a 2.5 min infusion. Additionally, 0.33 mg/kg was infused in 2.5 min at 15, 30, and/or 45 min after the end of the surgery if pain relief, assessed by the objective pain scale [OPS (13,14)], was not adequate (pain score > 4/10). Rescue medication with other analgesics was allowed 60 min after the start of the first administration of T. The number of patients that required 0, 1, 2, or 3 additional infusions of T was 42, 42, 13, and 7, respectively. Eight individuals received a single dose of T ranging from 0.45 to 2.8 mg/kg as rescue medication within the interval at which the second blood sample was taken (≥ 60 to 148 min after the start of the first infusion of T), and therefore that additional dosing information was taken into consideration.

Pharmacokinetic Data

A total number of 175 of T and 172 levels of M1 in plasma were available from 93 children. For each of those patients, one to three (2 ml) blood samples were withdrawn for determination of racemic T and M1. The first blood sample was taken within the first hour and before the first re-injection of T, and the rest in the interval from 2 to 6 h after the initial infusion. The samples were centrifuged and the plasma was separated and stored at −20°C until analysis.

Analytical Method

T and M1 were determined non-stereoselectively by GC and nitrogen-selective detection (15). Fused-silica columns of dimension 25m×0.32 mm I.D, coated with chemically bonded SE 30 were used. The operating conditions were: Injector T^a 250°C, detector T^a 300°C, column T^a was programmed from 100 to 240°C at 32°C/min. Gas flow rates were: helium, 60 cm/second; hydrogen 4 ml/min; air, 80 ml/min. The calibration curves with sample concentrations of 10 – 1,000 ng/ml for T and 5 –100 ng/ml for M1 were linear ($r > 0.997$). Precision and accuracy of the assay showed coefficient of variations < 8.5% for T and M1. Detection limit was 3 ng/ml.

Pharmacodynamic Data

Pain intensity was assessed by a trained nurse using the OPS at times equal to 15, 30, 45, 60, 120, 180, 240, 300 and 360 min after the start of the first infusion of T. OPS involves five items each of them measured with a three-category ordinal scale (0, 1, and 2): crying, movement, agitation, verbal evaluation, and increase in systolic blood pressure. The presence of adverse events together with the time at which the patients took the rescue medication were also recorded. For each of the variables the number of scores recorded at times 15–60 min ranged from 103 to 104. That number decreased to 65, 60, 58, 57 and 55 at times 120, 180, 240, 300 and 360 min, respectively, because once the subjects took the rescue medication the rest of their measurements were excluded from the analysis with the exception of those cases were tramadol was used as rescue medication (see below). The number of children that took rescue medication was 49 and the median (range) time to rescue medication was 75

(60–320) min. NSAIDS [diclofenac, ibuprofen, paracetamol, metamizole, and acetylsalicylic], and opiods [morphine, tramadol, codeine, and pethidine] were the drugs used for rescue medication.

Data Analysis

All analyses were performed under the population approach using the NONMEM version V (level 1.1) software (16). Selection between models was based on a number of criteria such as goodness-of-fit plots, precision of parameter estimates, and the minimum value of the objective function (OBJ; -2log likelihood) provided by NONMEM (see below). Results from the population analysis were expressed as model parameter estimates together with their corresponding 95th confidence intervals (CI) computed using the likelihood profiling method.

Pharmacokinetics

All observed plasma concentrations of T and M1 were fitted simultaneously and due to the sparse nature of the data, the first order estimation method implemented in NONMEM was used. The final model was rerun using the first order conditional estimation method with the INTERACTION option, however the run did not minimize successfully. A model was declared superior over the other nested model when the OBJ was reduced by 6.63 ($P < 0.01$) points between the two models.

The disposition of parent drug and metabolite was described with compartmental models. The apparent volume of distribution of M1 was assumed to be equal to the apparent volume of distribution of the central compartment of T (V), to make the model identifiable. Inter-patient variability was incorporated in the model exponentially. Residual variability was modelled additively. The significance of the off-diagonal elements of the Ω and Σ variance–covariance matrixes was explored. The stepwise generalised additive model (GAM) approach was used to identify the potential important covariates and their functional relationships with the parameters (17). The GAM approach was performed with Splus using the Xpose version 3.011 program (18). The covariates tested for significance are listed in Table I. Covariates selected during the GAM approach were then evaluated individually in NONMEM. The possibility of having two different sub-populations characterised by different population mean estimates at the level of the M1 formation clearance (CL_F) was explored fitting a mixture model to the data (19).

The visual predictive check was used to explore the selected model (20). First, one thousand new data sets as the original data were simulated. Second, concentrations were grouped using the following sampling times: (14 – 30), (> 30 – 45), (> 45 – 60), (> 120 – 180), (> 180 – 240), and (> 240 – 300) min. Third, for each of the simulated datasets and sampling time group, the median of the concentrations was computed and the distribution was represented as histogram together with the median concentration values corresponding to the original data.

The impact of the selected covariates on the plasma concentration *versus* time profiles of T and M1 was investigated by computer simulations. For the case of a continuous covariate, one thousand individuals were simulated for each of the values corresponding to the 5, 50, and 95th percentiles of the covariate in the studied population, assuming a single 2.5 min intravenous infusion of 20 mg of T.

Pharmacodynamics

In the current report the results obtained from the analysis of the crying and movement response variables are presented. The agitation response is not further described in this document since it was very similar to crying. Figure 1 shows in the upper panel the time course of the crying response where scores of 0, 1, and 2 correspond to the not crying, crying but consolable, and crying but inconsolable status, respectively. In the lower panel of Fig. 1 the time profiles of the movement response are shown where scores of 0, 1, and 2 correspond to none, restless and thrashing, respectively. For both responses, the 0, 1, and 2 scores can be related to no pain, moderate pain, and severe pain. For the case of verbal evaluation and increase in systolic blood pressure, it was not possible to find a model relating those response variables to drug exposure.

The time course of the crying and movement response variables was described using the LAPLACIAN estimation method with the LIKELIHOOD option. A decrease in OBJ of 3.84 points after the inclusion of an extra parameter or a covariate in the model, was considered significant ($P < 0.05$).

Response measurements were treated as ordered categorical data and analysed by logistic regression. The probability of obtaining a score lower than or equal to a particular grade m, in the i^{th} individual at time j^{th} [$P(Y_{ij} \leq m|\eta_i)$], where η_i is the individual random effect, is given by the expression: $\exp(L)/(1+\exp(L))$. The set of individual η is assumed to be

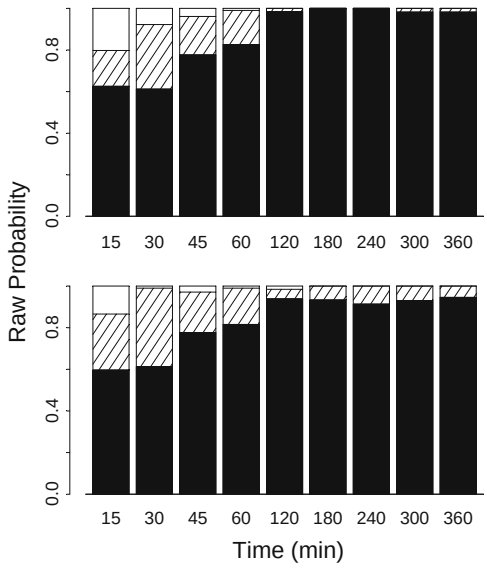

Fig. 1. Raw data for the analgesic response variables modelled during the analysis. Each *bar* is divided into regions proportional to the number of patients exhibiting the various scores. *Upper panel*, crying response: *Black*, score = 0 (not crying); *solid lines*, score = 1 (crying but consolable); *white*, score = 2 (crying but not consolable). *Lower panel*, movement response: *Black*, score = 0 (none); *solid lines*, score = 1 (restless); *white*, score = 2 (thrashing).

symmetrically distributed around 0 with variance ω^2. The probability of obtaining a certain m score $[P(Y_{ij} = m|\eta_i)]$ was expressed as: $P(Y_{ij} \leq m|\eta_i) - P(Y_{ij} \leq (m-1)|\eta_i)$. The logit ($L$) involves the contribution of baseline, drug, and time effects to the probability of obtaining a score lower than or equal to a particular score m as follows: $L = F_{Baseline} + H_{exposure} + G_{time} + \eta_i$. $F_{Baseline}$ defines the model describing the distribution of scores at baseline and has the form $\sum_{k=1}^{m} \beta_k$. The number of baseline parameters to be estimated is equal to the number of categories minus one, because $P(Y \leq 2)=1$. $H_{exposure}$ represents drug effects that were described as a linear or non-linear function (E_{MAX} model) of the plasma or effect site concentrations of T or M1 (21). Models exploring a pharmacodynamic interaction between T and M1 were also explored using the following expression: $H_{exposure} = SLP_T \times C_{e\_T} + SLP_{M1} \times C_{e\_M1}$, where SLP_T and SLP_{M1} are the slopes of the linear contribution of the effect site concentrations of T (C_{e_T}) and M1 (C_{e_M1}) to the effect. G_{time} represents pain progression and/or contribution of residual anaesthetic effects, and its shape and significance was evaluated by fitting different time-dependent models to the data.

Individual predicted plasma concentrations of T and M1 obtained from the selected population pharmacokinetic model were used during the analysis of the response data. For the 11 children without available pharmacokinetic information the typical population model predictions were used. Since only one random effect is estimated all covariates were tested in NONMEM.

Goodness-of-fit plots represent mean model predicted and mean raw data cumulative probabilities (both computed using time of measurement as group variable) *vs* time. The visual predictive check was again used to explore the model (20). Scores from one thousand datasets were simulated. For each simulated dataset and time of measurement the mean probability corresponding to each score was computed. Then, for each measurement time and score, the overall median value was calculated. Finally, the overall median values were plotted against the mean raw data probabilities.

RESULTS

Pharmacokinetic Modelling

Disposition of T and M1 in plasma was best characterised by a two-and a one-compartmental model, respectively. The inclusion of a second elimination pathway for T (CL_E) was significant ($P < 0.01$). Inter-patient variability was estimated for V, K_{12} (first order rate constant of distribution of T from the central to the peripheral compartment), CL_E, and for the apparent formation clearance of M1 (CL_F). Covariance was found to be significant ($P < 0.01$) between V and K_{12}. Only weight showed significant covariate effects on V and CL_E, respectively ($P < 0.01$). Covariate interactions between weight and age for V, between weight and height for CL_E, and allometric relationships did not improve the fit significantly ($P > 0.05$) (22,23). When a mixture model was fitted to the data, the estimated fraction of the poor metabolisers was higher than 30%, and the differences in the typical estimates of CL_F between fast and poor metabolizers were less than 50%.

Table II. Population Pharmacokinetics Estimates for T and M1

Parameter or covariate model	Estimate	Interpatient variability
$V(L) = V_{int} + V_{slp} \times \frac{Weight}{19.64^*}$	V_{int} = 3.12 (0.4–7) V_{slp} = 4.89 (1.75–11)	41 (17–60)
CL_F (l/h)	0.51 (0.21–1.2)	38 (26–71)
$CL_E(l/h) = CL_{E\_slp} \times \frac{Weight}{19.64^*}$	CL_{E_slp} = 14.7 (12.6–16.2)	28 (14–44)
K_{12} (L/h)	8.4 (5.1–12.6)	53 (30–60)
K_{21} (L/h)	1.76 (1.5–2.7)	NE
CL_{M1} (l/h)	3.52 (1.2–7.5)	NE
Correlation (η_V, η_{K12})	−0.78 (−0.03–0.3)	NA
Residual error_T (ng/ml)	43.01 (10–59)	NA
Residual error_M1 (ng/ml)	4.32 (2.7–6.3)	NA

Parameter estimates are listed together with their 95th confidence intervals [computed using the log-likelihood method] in parenthesis. Random effects are expressed as coefficient of variation (%). V, Apparent volume of distribution of the central compartment for T, CL_F apparent formation clearance of M1, CL_E, plasma clearance of T representing other routes of elimination that do not lead to formation of M1, K_{12} and K_{21} first order rates of distribution on T, CL_{M1} apparent plasma clearance of M1; η_V, and η_{K12}, individual random effects of V and K_{12}, respectively, *NE* not estimated, *NA* not applicable; * median value of weight corresponding to the children with pharmacokinetic information.

Population pk parameter estimates of the final model are listed in Table II, and results from model exploration are shown in Fig. 2. Figure 3 shows the individual model predicted profiles for ten patients chosen at random and receiving a single administration of *T*.

The model predicts an increase in V and CL_E of 0.25 l and 0.72 l/h, respectively, for a 1 kg increase in body weight. Estimates of the inter-patient variability in V and CL_E decreased from 52 to 41% and from 33 to 28% in the final model with respect to the basic population model, which represents a relative change in the degree of inter-patient variability of 32 and 18%, respectively. Figure 4 explores the covariate effects found for weight on V and CL_E. Weight appears to have a clear effect on the entire plasma concentration *vs* time profiles for both T and M1.

Pharmacodynamic Modelling

Crying Response

Relating drug effects with the predicted effect site concentrations of T or M1 provides significant ($P < 0.01$) decreases in OBJ with respect to the models using the predicted plasma concentrations of T or M1. The difference in OBJ indicates that the effect site concentrations of M1 are a better response descriptor than T ($P < 0.01$). The presence of time effects and an interaction between T and M1 was not supported by the data ($P > 0.05$). An E_{MAX} model did not lead to any improvement in the fit with respect to the linear model ($P > 0.05$). Including weight as a covariate was significant ($P < 0.01$), and the estimate of ω^2 decreased from 3.06 to 2.62. In the final model the logit was expressed as follows: $L = \sum_{k=1}^{m} \beta_k + SLP \times C_{e\_MI} + \theta_{wgt} \times weight / 19.8$, where SLP is the parameter describing the linear increase in L as a function

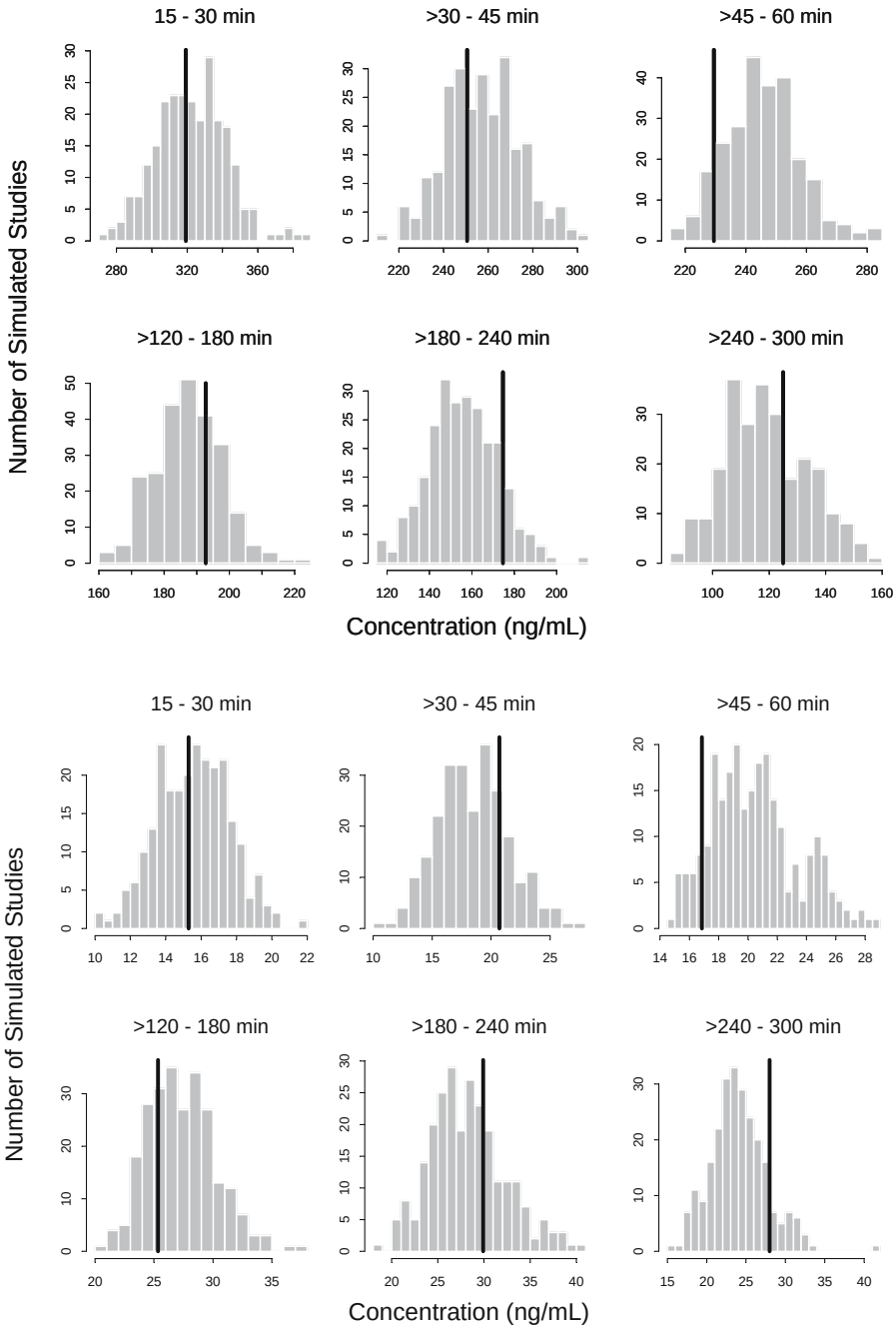

Fig. 2. Results from the visual predictive check. The six upper panels correspond to tramadol and the rest to the metabolite. In each panel the histrogram represents the distribution of the median concentrations computed for each of the simulated datasets at each time interval, and the vertical *black solid line* represents the median concentration values computed from the raw data.

of C_{e_M1}; θ_{wgt} is the parameter scaling the effect of weight, and 19.8 is the mean value of weight in the studied population. The covariate model predicts at baseline an approximately 3% typical increase in $P(Y = 0)$ for a 1 kg increase in body weight. Table III shows the population model estimates corresponding to the final model. Figure 5 (upper panels) shows a goodness of fit plot (left) and the results from the model exploration exercise (right), confirming that the model was supported by the data.

Movement Response

The difference in OBJ indicates that the effect site concentrations of T are the best response descriptor ($P < 0.01$). The presence of time effects and an interaction between T and M1 was not supported by the data ($P > 0.05$). An E_{MAX} model did not lead to any improvement in the fit with respect to the linear model ($P > 0.05$). Covariates did not show significant effects ($P > 0.05$). Table III shows also the population

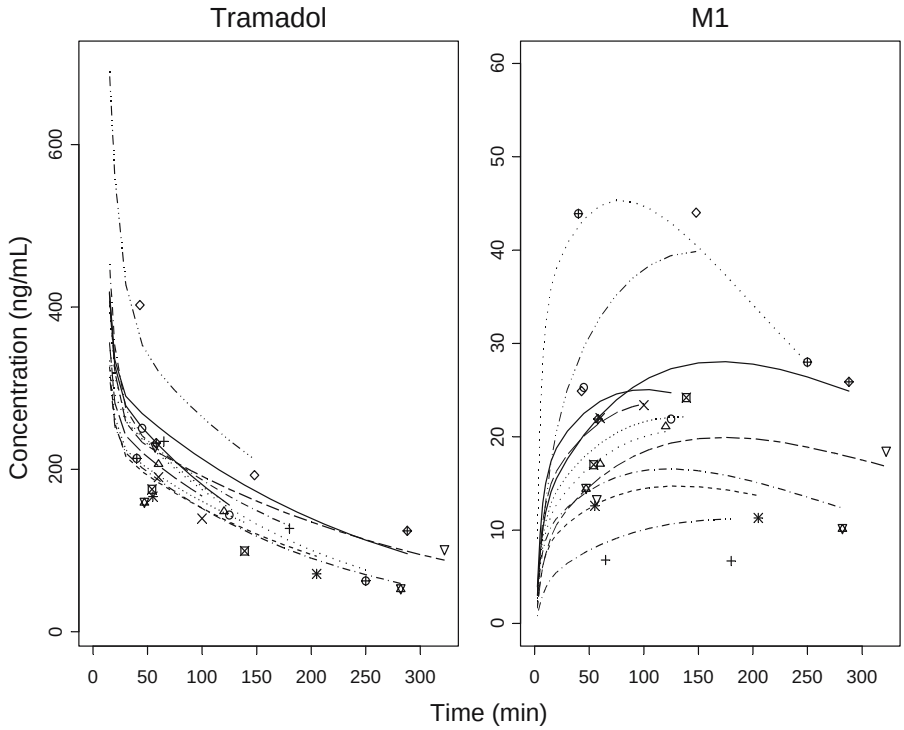

Fig. 3. Plasma concentrations *vs* time profiles of T (*left panel*) and M1 (*right panel*) corresponding to ten children selected at random and receiving only the first infusion of T. *Symbols*, observations; *lines*, individual model predictions.

model estimates corresponding to the final model. Figure 5 (lower panels) shows a goodness of fit plot (left) and the results from the model exploration exercise (right), confirming that the model was supported by the data.

Adverse Events

A total of 20 vomit events were recorded in 15 children during the span of the study. Twelve of those events occurred

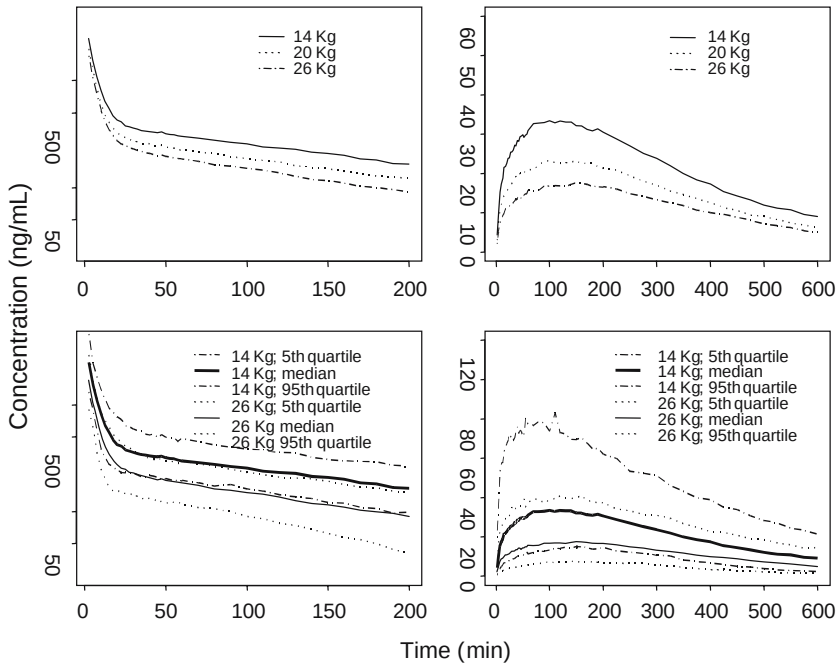

Fig. 4. *Upper panels*: Typical (median) pharmacokinetic profiles for T and M1 in children with body weight of 14, 20 and 26 kg. *Lower panels*: Typical (median) pharmacokinetic profiles and 90% prediction intervals (area covered by the 5 and 95th percentiles) as a function of weight. Median and quartiles are the result of one thousand simulations where a single 2.5 min iv infusion of 20 mg of T was assumed.

Table III. Population Pharmacodynamic Estimates after Administration of T

Parameter	Crying	Movement
Logit model	$L = \sum_{k=1}^{m} \beta_k + SLP \times C_{e-M1} + \frac{Weight}{19.8}$	$L = \sum_{k=1}^{m} \beta_k + SLP \times C_{e-T}$
β_1	−0.3 (1.4– −2.1)	1.66 (0.62–2.75)
β_0	−2.4 (−0.75– −4.3)	−1.25 (−2.25– −0.35)
SLP (ml • ng^{-1})	0.26 (0.16–0.85)	0.035 (0.027–0.052)
k_{e0} (min^{-1})	7 (1.4–14) × 10^{-3}	3.5 (1.5–5.2) × 10^{-3}
θ_{wgt}	2.9 (1.2–4.7)	–
ω^2	2.6 (1.3–4.8)	3.6 (2.25–6.25)

L Logit, 95th confidence intervals in parenthesis; β_k (k = 1,0) set of baseline parameters, *SLP* parameter describing the linear increase in the logit as a function of the effect site concentrations of M1, C_{e_M1} (crying response) or tramadol, C_{e_T} (movement response), k_{e0} first order rate constant governing drug or metabolite distribution from plasma to the effect site, θ_{wgt} parameter scaling the effect of weight, ω^2 population variance.

at times between 16 and 80 min after the start of the initial infusion of T, and the rest between 130 and 317 min. The mean predicted T and M1 plasma concentrations (ng/ml) at the time of the event were within the range of T and M1 concentrations predicted for the rest of patients that did not experience vomiting.

DISCUSSION

A review of the properties of T in perioperative pain concluded that T provided effective analgesia in children and in adults (24). Moreover, results after oral administration of T to 81 post-surgical children (7–16 years) at the moment of the transition from patient-controlled administration of morphine to oral analgesics indicate a certain exposure-response relationship, since patients receiving 2 mg/kg of T required half of the rescue medication given in the 1 mg/kg dose group (25). At this stage, to get a better understanding of the *in vivo* effects of T, and improve individual dose selection, a population pk/pd model is needed. The current study represents the first population pk/pd analysis of T in children.

During the population pharmacokinetic analysis the first order estimation method was used and therefore is likely that significant alpha error could be expected and a change in successive objective function values of 6.63 points possibly is not associated with $P < 0.01$ (26), however the decrease in the minimum value of the objective function was greater than 30 points for all the comparisons described in the results section.

Disposition of T in plasma was best characterised by a two compartment body model and the elimination of M1 was limited by its rate of formation. The estimate of V_{SS} (47.8 l) was higher than the physiological water volume and equiv-

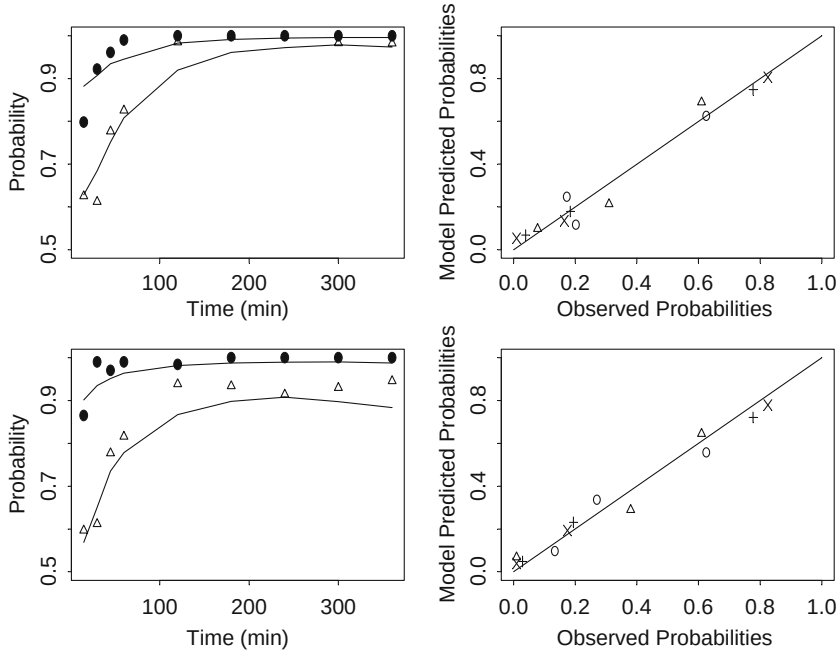

Fig. 5. *Left panels*: Mean raw data (*symbols*) and typical model predicted (*lines*) cumulative probabilities *vs* time profiles. *Solid circles* represent $P(Y \leq 1)$ and *triangles* $P(Y = 0)$. *Right panels*: Results from the visual predictive check. Overall medians computed from one thousand simulated datasets are plotted against the corresponding medians obtained from the raw data. *Symbols* reflect different group times. *Upper panels* correspond to the crying response and lower panels to movement.

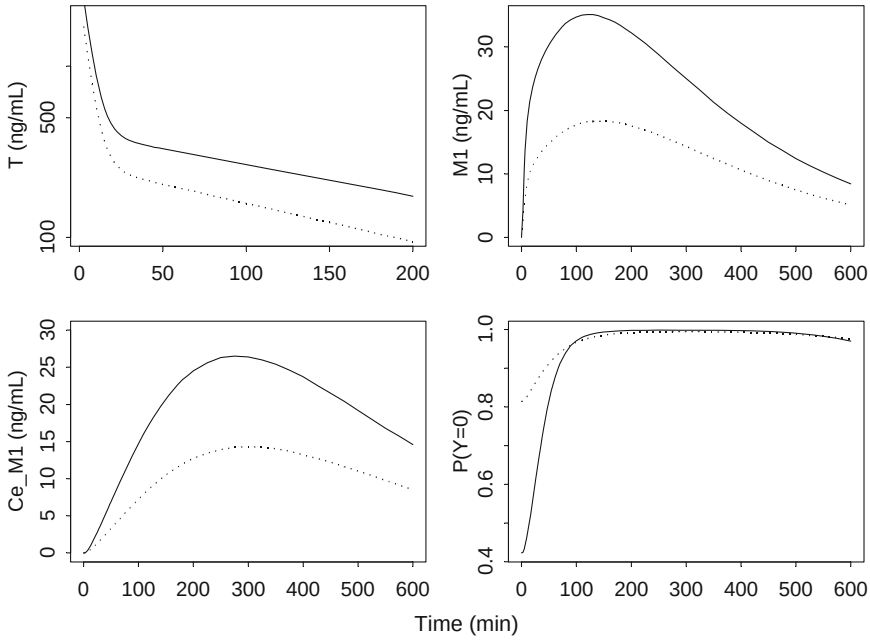

Fig. 6. Typical model predicted time course of T in plasma (*upper left panel*), M1 in plasma (*upper right panel*), M1 in the effect site (*lower left panel*) and $P(Y = 0)$ corresponding to the crying response [*lower right panel*] as a function of body weight: *solid*, 14 kg; *dashed*, 26 kg. A 2.5 min intravenous administration of T at the dose of 20 mg was assumed. Predictions correspond to the model developed for the crying response.

alent to 2.43 l/kg, a value in the range of the estimates obtained in healthy children and adults (9,27,28), and in preclinical experiments with adult rats [3.9 l/kg (10–12)]. Total plasma clearance of T (0.77 l/h/kg) was estimated with a value similar to that reported in young infants (0.51 l/h/kg) and in adults (0.34–0.5 l/h/kg) (9,28). The apparent estimate of CL_E was higher than the one corresponding to CL_F, however it cannot be confirmed than formation of M1 represents a minor elimination pathway of T, due to the fact that it is not possible to determine the absolute amount of metabolite formed. CL_F and CL_E correspond actually to the value of $f_{M1} \times CL$ and $(1-f_{M1}) \times CL$, respectively, where f_{M1} is the fraction of the administered dose of T which is transformed from the parent compound to M1. In fact, regarding to the difference in the ratio between CL_F and CL shown in the current manuscript (~3%) with respect to the ratio reported in reference 9 (~43%) we think that such discrepancy can be partly explained taking into account the differences in the values used for the apparent volume of distribution of the metabolite (8L *vs* 224L) to avoid the identifiability problem in the pharmacokinetic model. However there are some evidences in the literature suggesting that CL_F is not one of the main routes of elimination of T since results obtained from situations where CL_F was decreased by co-administration of a CYP2D inhibitor (12) or by the presence of poor metabolizers (29) showed that the total plasma clearance of T was modified to a minor degree.

Weight was the only individual characteristic showing significant covariate effects and eliciting a 12 and a 6% reduction in the inter-patient variability of V and CL_E, respectively.

T is metabolized by the CYP2D6 enzyme for which genetic polymorphism affecting 5–10% of Caucasian population has been reported. Since CL_E is higher than CL_F, deficiencies in CYP2D6 activity would affect mainly to M1 disposition. Genotyping and phenotyping was not performed, and a pure statistical approach based on mixture models was undertaken. That approach for example has allowed to identify two subpopulations in the distribution of pharmacokinetic, and pharmacodynamic parameters (30,31). In our case, the presence of poor metabolizers could not be detected. This result was in part expected on the basis of the estimate obtained for the degree of inter-patient variability in CL_F (28%), which could be considered rather low in the case of a population including poor metabolizers. In addition the visual inspection of the distribution of individual estimates of CL_F did not reveal a bimodal distribution. The pk/pd model presented has been developed using racemic concentrations. However, since there are data in the literature that show that at least for the case of extensive metabolizers, the enantiomers of T and M1 have similar kinetics (29), we do think that the proposed model provides a fair description of the pk characteristics of T and M1 in children.

During the analysis of the response data, it was found that models relating drug effects with effect site concentrations behaved significantly better. Since the process of distribution from plasma to the effect site appeared to be unaffected by the covariates explored, the effect site concentration *vs* time profiles will reflect the influence of weight on the kinetics of T and M1 in plasma [see Fig. 6 (lower left panel)]. After a single 2.5 min infusion of T, maximum T and M1 concentrations in the effects site appear at 4–5 h. The times to reach the equilibrium between plasma and biophase for T and M1 were 9 and 4.2 h, respectively. These values are in the range of those reported for morphine (14 h) (32), shorter than morphine-6-glucuronide (38.5 h) (32), and larger than methadone (1 h) (33). However, it should be taken into

consideration that the duration of the study was 6 h which might has an implication on the accuracy of the model estimates of k_{e0} (first order rate constant responsible of drug distribution between plasma and biophase).

Crying response was best described using model predicted concentrations of M1 in the effect site, whereas modelling of the movement response required the use of T. These results resemble the known pharmacological properties of T where both the parent compound and the metabolites seem to contribute to the analgesic response (34,35). Therefore the crying and movement responses might be reflecting the contribution of the μ-opioid and non-opioid pharmacodynamic properties of the components of T, respectively. It should be taken into account that the additive interaction model used considers the effects of T and M1 as being conditionally independent. In order to explore in more detail the nature of the interaction between T and M1 the following expressions were fitted to the crying and movement responses, respectively: $H_{\text{exposure}} = SLP_{\text{M1}} \times C_{\text{e\_M1}} \times (1+SLP_{\text{T}} \times C_{\text{e\_T}})$ and $H_{\text{exposure}} = SLP_{\text{T}} \times C_{\text{e\_T}} \times (1 + SLP_{\text{M1}} \times C_{\text{e\_M1}})$. In both cases the models did not improve the fits significantly ($P > 0.05$).

Inclusion of a placebo group was not possible for ethical reasons. To describe the possible time course of pain in absence of T, the concept of the "virtual drug" applied to the pharmacodynamics of midazolam in intensive care patients recovering from coronary artery bypass grafting was used (36). The "virtual drug" was assumed to be (i) absent at the time of skin closure with a non-linear increase with time (resembling the wane of post-surgical pain) or (ii) present in its highest concentration at the time of skin closure with a decline over time (residual anesthetic effects). Models including the virtual drug concept were not supported by the data but weight elicited significant effects in the crying response at baseline. There is the possibility that the residual anaesthetic effect disappears at a rate at which is a function of body weight. In fact, an increase in the terminal half life in the case of alfentanyl was associated with body weight (37). Children with higher weight were associated with a higher probability of pain relief just after the end of surgery, however such covariate effects are probably not generalizable and can only be made relative to the current study. Figure 6 (lower right panel) shows the typical predicted time course of $P(Y = 0)$ as a function of weight for the case of the crying response obtained from the final pk/pd model. It can be observed that, despite the higher M1 concentrations in the effect site for the typical 14 kg child (Fig. 6, lower left panel), the time to achieve a 0.9 probability of complete pain relief is prolonged from 50 (value predicted for the 26 kg child) to 80 min.

In a study carried out in adults (38), mean racemic T and M1 plasma concentrations of 590 and 84 ng/ml, respectively, were associated with an adequate degree of pain relief. In the current study effect site concentrations of 15 ng/ml of M1 and 100 ng/ml of T are associated with an adequate control of pain. In Fig. 6 it can be observed that those levels in the effect site are associated with plasma concentrations of 20–30 ng/ml of M1 and 200–300 ng/ml of T (plot not shown), suggesting that the M1 and T requirements are lower in the pediatric population.

Dropouts due to rescue medication represent non-random missingness. Although, a dropout model has been used in the past to account for this phenomenon (39), in the current analysis a simpler approach was taken assuming that the time to rescue medication (TR) depends only on the observed response scores, and therefore TR does not contain information about the observed scores (40).

To summarize, the analgesic response elicited after T administration was described successfully with a population pk/pd model. Effect site concentrations of M1 were found to be the best predictors of the crying response. Weight was found to have a significant effect on the crying response at baseline, predicting an approximately 3% typical increase in $P(Y = 0)$ for a 1 kg increase in body weight. Movement was best correlated with T in the effect site. Typical steady-state plasma concentration levels of M1 and T of 15 and 100 ng/ml, respectively, were associated with a 95% probability of adequate analgesia. The response variables investigated give further evidence that not only the opioid effects of the metabolite are relevant, also the non-opiod effects of tramadol seem to give a significant contribution in its clinical use.

ACKNOWLEDGMENT

This work was supported by Grünenthal GmbH, Aachen, Germany.

REFERENCES

1. L. J. Scott and C. M. Perry. Tramadol: a review of its use in perioperative pain. *Drugs* **60**:139–176 (2000).
2. C. H. Wilder-Smith, J. Schimke, B. Osterwalder, and H. J. Senn. Oral tramadol, a mu-opioid agonist and monoamine reuptake-blocker, and morphine for strong cancer-related pain. *Ann. Oncol.* **5**:141–146 (1994).
3. W. D. Paar, P. Frankus, and H. J. Dengler. The metabolism of tramadol by human liver microsomes. *Clin. Investig.* **70**:708–710 (1992).
4. W. D. Paar, S. Poche, J. Gerloff, and H. J. Dengler. Polymorphic CYP2D6 mediates O-demethylation of the opiod analgesic tramadol. *Eur. J. Clin. Pharmacol.* **53**:235–239 (1997).
5. C. Gillen, M. Haurand, D. J. Kobelt, and S. Wnendt. Affinity, potency and efficacy of tramadol and its metabolites at the cloned human mu-opioid receptor. *Naunyn Schmiedebergs Arch Pharmacol.* **362**:116–121 (2000).
6. D. M. Halfpenny, L. F. Callado, S. E. Hopwood, T. A. Bamigbade, R. M. Langford, and J. A. Stamford. Effects of tramadol stereoisomers on norepinephrine efflux and uptake in the rat locus coeruleus measured by real time voltammetry. *Br. J. Anaesth.* **83**:909–915 (1999).
7. M. Ch. Frink, H. H. Hennies, W. Englberger, M. Haurand, and B. Wilffert. Influence of Tramadol on neurotransmitter systems of the rat brain. *Arzneim.-Forsch./ Drug Res.* **46**:1029–1036 (1996).
8. C. A. Fairbanks and G. L. Wilcox. Spinal antinociceptive synergism between morphine and clonidine persists in mice made acutely or chronically tolerant to morphine. *J. Pharmacol. Exp. Ther.* **288**:1107–1116 (1999).
9. K. Allegaert, B. J. Anderson, R. Verbesselt, A. Debeer, J. de Hoon, H. Devlieger, J. N. Van Den Anker, and D. Tibboel. Tramadol disposition in the very young: an attempt to assess *in vivo* cytochrome P-450 2D6 activity. *Br. J. Anaesth.* **10**:1–9 (2005).
10. M. Valle, M. J. Garrido, J. M. Pavón, R. Calvo, and I. F. Trocóniz. Pharmacokinetic-pharmacodynamic modeling of the antinociceptive effects of main active metabolites of tramadol, (+)−O-desmethyltramadol and (−)−O-desmethyltramadol, in rats. *J. Pharmacol. Exp. Ther.* **293**:646–653 (2000).

11. M. J. Garrido, M. Valle, M. A. Campanero, R. Calvo, and I. F. Trocóniz. Modeling of the *in vivo* antinociceptive interaction between an opiod agonist, (+)−O-desmethyltramadol, and a monoamine reuptake inhibitor, (−)−O-desmethyltramadol, in rats. *J. Pharmacol. Exp. Ther.***295**:352–359 (2000).
12. M. J. Garrido, O. Sayar, C. Segura, J. Rapado, M. C. Dios-Viéitez, M. J. Renedo, and I. F. Trocóniz. Pharmacokinetic/pharmacodynamic modeling of the antinociceptive effects of (+)−tramadol in the rat: role of Cytochrome P450 2D activity. *J. Pharmacol. Exp. Ther.***305**:710–718 (2003).
13. L. M. Broadman, L. J. Rice, and R. S. Hannallah. Evaluation of an objective pain scale for infants and children. *Regional Anesthesia***13**:45 (1988).
14. J. Norden, R. Hannallah, and P. Getson. Reliability of an objective pain scale in children. *Anesth. Analg.***72**:S199 (1991).
15. R. Becker and W. Lintz. Determination of tramadol in human plasma by capillary gas chromatography with nitrogen-selective detection. *J. Chromatogr.* **25**:213–220 (1986).
16. S. L. Beal and L. B. Sheiner. *NONMEM Users Guides*. San Francisco: NONMEM Project Group, University of California at San Francisco, 1992.
17. J. W. Mandema, D. Verotta, and L. B. Sheiner. Building population pharmacokinetic–pharmacodynamic models. I. Models for covariate effects. *J. Pharmacokinet. Biopharm.* **20**:511–528 (1992).
18. E. N. Jonsson and M. O. Karlsson. Xpose: An Splus based population pharmaco-kinetic/pharmacodynamic model building aid for NONMEM. *Comput. Methods Programs Biomed.* **58**:51–64 (1999).
19. G. Alván, P. Bechtel, L. Iselius, and U. Gundert-Remy. Hydroxylation polymorphisms of debrisoquine and mephenytoin in Europeans populations. *Eur. J. Clin. Pharmacol.* **39**:533–537 (1990).
20. Holford N. The visual predictive check-superiority to standard diagnostic (Rorschach) plots (http://www.page-meeting.org/default.asp?abstract=738). 14th meeting of the Population Approach Group in Europe. Pamplona, Spain (2005).
21. L. B. Sheiner, D. R. Stanski, S. Vozeh, R. D. Miller, and J. Ham. Simultaneous modeling of pharmacokinetics and pharmacodynamics: application to d-tubocurarine. *Clin. Pharmacol. Ther.* **25**:358–371 (1979).
22. B. J. Anderson, G. A. Woollard, and N. H. G. Holford. A model for size and age changes in the pharmacokinetics of paracetamol in neonates, infants and children. *Br. J. Clin. Pharmacol.* **50**:125–134 (2000).
23. N. H. G. Holford. A size standard for pharmacokinetics. *Clin. Pharmacokinet.* **30**:329–332 (1996).
24. H. F. Miranda and G. Pinardi. Antinociception, tolerance and physical dependence: comparison between morphine and tramadol. *Pharmacol. Biochem. Behav.* **61**:357–360 (1998).
25. J. C. Finkel, J. B. Rose, M. L. Schmitz, P. K. Birmingham, G. A. Ulma, J. B. Gunter, A. Cnaan, C. J. Cote, R. A. Medve, and M. S. Schereiner. An evaluation of the efficacy and tolerability of oral tramadol hydrochloride tablets for the treatment of postsurgical pain in children. *Anesth. Analg.* **94**:1469–1473 (2002).
26. U. Wahlby, E. N. Jonsson, and M. O. Karlsson. Assessment of actual significance levels for covariate effects in NONMEM. *J. Pharmacokinet Pharmacodyn* **28**:231–252 (2001).
27. C. R. Lee, L. McTavish, and E. M. Sorkin. Tramadol. A preliminary review of its pharmacodynamic and pharmacokinetic properties, and therapeutic potential in acute and chronic pain sates. *Drugs* **46**:313–340 (1993).
28. B. V. Murthy, K. S. Pandya, P. D. Booker, A. Murray, W. Lintz, and R. Terlinden. Pharmacokinetics of tramadol in children after iv or caudal epidural administration. *Br. J. Anaesth.* **84**:346–349 (2000).
29. L. Poulsen, L. Arendt-Nielsen, K. Brøsen, and S. H. Sindrup. The hypoalgesic effect of tramadol in relation to CYP2D6. *Clin. Pharmacol. Ther.* **60**:636–644 (1996).
30. B. Facca, B. Frame, and S. Triesenberg. Population pharmacokinetics of ceftioxime administered by continuous infusion in clinically ill adult patients. *Antimicrob. Agents Chemother.* **42**:1783–1787 (1998).
31. E. Comets, F. Mentré, P. Grass, R. Kawai, P. Marbach, and J. Vonderscher. Population pharmacodynamic analysis of octreotide in acromegalic patients. *Clin. Pharmacol. Ther.* **73**:95–106 (2003).
32. C. Skarke, J. Darimont, H. Schmidt, G. Geisslinger, and J. Lotsch. Analgesic effects of morphine and morphine-6-glucuronide in a transcutaneous electrical pain model in healthy volunteers. *Clin. Pharmacol. Ther.* **73**:107–121 (2003).
33. C. E. Inturrisi, R. K. Portenoy, M. B. Max, W. A. Colburn, and K. M. Foley. Pharmacokinetic–pharmacodynamic relationships of methadone infusions in patients with cancer pain. *Clin. Pharmacol. Ther.* **47**:565–577 (1990).
34. R. B. Raffa and E. Friderichs. The basic science aspect of tramadol hydrochloride. *Pain Rev.* **3**:249–271 (1996).
35. S. Grond, T. Meuser, D. Zech, U. Hennig, and K. A. Lehmann. Analgesic efficacy and safety of tramadol enantiomers in comparison with the racemate: a randomised, double-blind study with gynaecological patients using intravenous patient-controlled analgesia. *Pain* **62**:313–320 (1995).
36. J. Somma, A. Donner, K. Zomorodi, R. Sladen, J. Ramsay, E. Geller, and S. L. Shafer. Population pharmacodynamics of midazolam administered by target controlled infusion in SICU patients after CABG surgery. *Anesthesiology* **89**:1430–1443 (1998).
37. P. O. Maitre, S. Vozeh, J. Heykants, D. A. Thomson, and D. R. Stanski. Population pharmacokinetics of alfentanil: the average dose-plasma concentration relationship and interindividual variability in patients. *Anesthesiology* **66**:3–12 (1987).
38. S. Grond, T. Meuser, H. Uragg, H. J. Stahlberg, and K. A. Lehmann. Serum concentrations of tramadol enantiomers during patient-controlled analgesia. *Br. J. Clin. Pharmacol.* **48**:254–257 (1999).
39. L. B. Sheiner. A new approach to the analysis of the analgesic drug trials, illustrated with bromfenac data. *Clin. Pharmacol. Ther.* **56**:309–322 (1994).
40. L. B. Sheiner and J. L. Steimer. Pharmacokinetic/pharmacodynamic modeling in drug development. *Annu. Rev. Pharmacol. Ther.* **40**:67–95 (2000).